Published in final edited form as:
Small. 2009 July ; 5(14): 1637–1641. doi:10.1002/smll.200801647.

Functionalized Nanoparticles with Long-Term Stability in Biological Media**

Chen Fang, **Narayan Bhattarai**, **Conroy Sun**, and **Miqin Zhang***
Department of Materials Science and Engineering, University of Washington, Seattle, WA 98195 (USA)

Keywords

Nanotechnology; Stability; Nanoparticles; Nanomedicine; Surface modification

Nanoparticles have been extensively studied in recent years due to their unique optical, magnetic, or chemical properties.[1-4] While many synthetic methods have been investigated, an effective way to produce ultrafine and monodisperse nanoparticles with controllable sizes is thermal decomposition of precursors in organic solvents at high temperature.[5,6] In this approach, nanoparticles are stabilized by hydrophobic coatings and as a result, the as-synthesized nanoparticles can not be dispersed in aqueous solutions. In biomedical applications, nanoparticles have to be hydrophilic and maintain a superior stability in biological media. For advanced biomedical applications of nanoparticles (e.g., *in vivo* diagnostics and therapy), additional requirements such as minimization of non-specific uptake by reticulo-endothelial systems (RES) must be imposed in order to achieve long blood circulation time and high diagnostic or therapeutic efficiency.[7] In addition, the surface of the nanoparticle should possess functional groups for further conjugation of targeting ligand or therapeutic agents. Commonly used modification strategies for coating hydrophobic nanoparticles with hydrophilic polymers include ligand exchange,[8] micelle encapsulation,[9] and covalent bonding.[10] [11] Particularly, hydrophilic poly(ethylene glycol) (PEG) have been the focus of research as an effective coating materials for nanoparticles[2,12-15] due to its ability to resist protein fouling and provide steric hindrance preventing nanoparticle from aggregation.[12,16,17] Typical examples include coating PEG on hydrophobic nanoparticles via ligand exchange in which dopamine linked PEG replaces oleylamine & oleic acid on the particle [18] and coating PEG on iron oxide nanoparticles in situ via covalent bonding during the aqueous co-precipitation process.[10] Despite the advances made with those methods, the challenge remains in producing a highly stable polymeric coating on nanoparticles and retaining the long-term stability of functionalized nanoparticles in biological-relevant media.

Here, we present a robust surface engineering approach to produce ultrafine, monodisperse, hydrophilic and functionalized oxide nanoparticles that display long-term colloidal stability in biological media and low non-specific uptake by macrophage cells. We demonstrated this approach with iron oxide nanoparticles as our model system. Due to their superparamagnetic properties and excellent biocompatibility, iron oxide nanoparticles have been extensively studied for biomedical applications including magnetic resonance imaging (MRI), cell labeling and tracking, and targeted therapeutic delivery.[1,3,19]

**The work was supported by a grant (R01CA119408) from the National Cancer Institute, the National Institute of Health.

* mzhang@u.washington.edu.

Supporting Information is available on the WWW under http://www.small-journal.com or from the author.

The chemical processes for the surface modification of the nanoparticle are illustrated in Scheme 1. The oleic acid-coated nanoparticles (NP-OA) were synthesized via thermal decomposition of iron oleate complex.[5] To render the nanoparticles hydrophilic, the NP-OAs were reacted with triethoxysilylpropylsuccinic anhydride (SAS) to form SAS-coated nanoparticles (NP-SAS) via a ligand-exchange and condensation process. Aminefunctionalized PEG was attached to NP-SAS via *N,N′*-dicyclohexylcarbodiimide (DCC) mediated coupling reaction to yield PEGylated nanoparticles (NP-SAS-PEG-NH_2). NP-SASPEG-NH_2 bears amine groups at the free termini of PEG chains allowing for further conjugation with bioactive molecules or ligands. The PEG coating also serves to prevent nanoparticles from agglomeration and protein adsorption.

TEM images showed that both NP-OA and NP-SAS-PEG-NH_2 were spherical and well dispersed, with a core size of ~12 nm (Fig. 1a). No aggregation of NP-SAS-PEG-NH_2 was observed, indicating that no inter-particle crosslinking occurred during the ligand exchange and PEG modification. Nanoparticle surface modification was confirmed by FTIR (Fig. 1b) and XPS (Figs. S1 and S2). The IR spectra of oleic acid coated nanoparticles exhibit the characteristic C-H stretch bands of methyl and methylene groups at 2930 and 2849 cm^{-1} and surface-complexed carbonyl stretch peaks at 1553 and 1433 cm^{-1} (Fig. 1b).[20] After the surface modification of nanoparticles with SAS, the Si-O-R vibrational bands, including a broad peak around 1031 cm^{-1} and a minor peak at 1188 cm^{-1}, were observed, indicating the formation of complex siloxane bonds. The relative intensity of surface-complexed carbonyl bands increased, compared to oleic acid-coated NPs, indicative of successful SAS attachment. The absence of characteristic anhydride peaks at 1850–1800 cm^{-1} and 1790–1740 cm^{-1}, [21] suggesting that these groups were either hydrolyzed or bonded to the iron oxide surface. After the surface modification of NP-SAS with amine-functionalized PEG, multiple bands at 1458, 1346, 1244, 1112 and 949 cm^{-1} were observed, corresponding to the different vibrational modes of PEG's C-O-C bonds.[3] The bands at 1642 and 1559 cm^{-1} can be assigned to either primary amine groups or mono-substituted amide, indicating the successful covalent attachment of PEG on the free carboxyl groups of NP-SAS. We determined the number of reactive amine groups on nanoparticles by quantifying pyridine-2-thione following reaction with *N*-succinimidyl 3-(2-pyridyldithio)propionate (SPDP).[22] We found that the number of amine groups on each nanoparticle is ~70, which is twice as much as those in an alternative nanoparticle system reported in our previous studies.[15] As the number of amine groups is proportional to the number of PEG chains, this result also suggests the formation of a high density PEG coating on the surface of the nanoparticle.

The hydrodynamic sizes of NP-OA in toluene and NP-SAS-PEG-NH_2 in phosphate-buffered saline (PBS) were determined to be 18 nm and 38 nm, respectively, by dynamic light scattering (Fig. 2a). The size increase (~20 nm) of the NP-SAS-PEG-NH_2 compared to NPOA can be attributed to the PEG (MW = 2,000) coating and the water molecules associated to PEG, comparable to the reported value.[9]

A significant challenge in application of nanoparticles is to retain their stability in application-associated environments. Aiming at biomedical applications, we evaluated the colloidal stability of NP-SAS-PEG-NH_2 by suspending the nanoparticles in three commonly used biological media: Dulbecco's phosphate-buffered saline (PBS), Dulbecco's modified eagle's medium (DMEM) with 10% of fetal bovine serum (FBS), and pure FBS. No significant size change was observed after incubation of the nanoparticles in these media for at least 15 days (Fig. 2b), demonstrating excellent colloidal stability of our nanoparticles under various culture media. We shelved the nanoparticles for 5 months in cell culture media and observed no apparent size increase or any particle precipitation.

Nanoparticles are generally electrically charged through additional surface coating to achieve their colloidal stability in solutions by electrostatic repulsive forces. However, electrostatically stabilized nanoparticles are prone to aggregation in biological media due to neutralization of the surface charge by ionic species present in the media. Additionally, charged nanoparticles tend to adsorb proteins in biological media through electrostatic interaction. The fouling of proteins on the surface of nanoparticles leads to gradual increase of the particle size and eventually to particle precipitation.[23] The prolonged colloidal stability exhibited by our nanoparticles in biological media (Fig. 2b) may be attributed to the presence of the highly dense and stable PEG coating. Hydrophilic PEG coatings have been shown to resist protein fouling and provide steric hindrance preventing nanoparticles from aggregation.[2] This highly stable PEG coating was formed as a result of strong affinity of SAS to oxide surfaces and the formation of silanol-silanol bridges or siloxane bonds between PEG chains (Fig. S1) in the current reaction scheme. Additionally, the amphiphilic nature of the PEG coating allows the PEGylated nanoparticles to be well dispersed in a wide range of organic solvents.

The amine groups presented at the free termini of the PEG chains on NP-SAS-PEG-NH_2 are designed to conjugate a variety of biomolecules. Here we tested this functionality with a cyclic arginine-glycine-aspartic acid (RGD) peptide with amine end groups. The RGD has a high affinity to $a_v\beta_3$ integrins highly expressed on the luminal surface of the endothelia cells only during angiogenesis and is commonly used as a targeting ligand for tumor vasculature[3]. We immobilized the sulfhydryl-functionalized cyclic peptide c(RGDyC) on nanoparticles by reacting its sulfhydryl groups with NP-SAS-PEG-NH_2 modified with succinimidyl iodoacetate (SIA) to form stable thioether linkages between RGD and nanoparticles. Successful immobilization of RGD on the particle was conformed by FTIR (Fig. S3). NPSAS-PEG-RGD has a hydrodynamic size of 53 nm after the three-day storage (Fig. 2a) and thereafter retained excellent colloidal stability in a DMEM cell culture medium for at least 12 days (Fig. 2b). It should be noted that a widely-used approach to conjugate ligands on PEG functionalized nanoparticles, the (1-Ethyl-3-[3-dimethylaminopropyl]carbodiimide) (EDC) crosslinking, is not appropriate for nanoparticles bearing both amine and carboxyl groups due to the potential crosslinking between the two groups. To use EDC crosslinking, one of the two groups needs to be temporarily blocked by a protective group. The protective group can be removed after the ligand is conjugated by EDC crosslinking.

Another challenge in production and use of nanoparticles for biomedical application, especially for *in vivo* application, is the ability to minimize non-specific uptake by macrophage cells. To evaluate the ability of our nanoparticles to resist the uptake by macrophage cells, the nanoparticles were incubated with mouse monocyte macrophage cells – RAW264.7 at the concentration of 10 μgFe/mL. Both NP-SAS-PEG-NH_2 and the conjugate - NP-SAS-PEG-RGD were evaluated while dextran-coated iron oxide nanoparticles were tested at the same conditions for comparison. The results (Fig. 3) showed that both NP-SAS-PEGNH_2 and NP-SAS-PEG-RGD achieved more than 75% reduction in overall intracellular iron content compared to dextran-coated nanoparticles, and the internalization of above-mentioned nanoparticles is negligible (less then 0.05 pg Fe/cell) after compared to background iron level (i.e., “Cells Only”).

To ensure that the iron oxide nanoparticles retain sufficient magnetism after surface coating, we tested the magnetic property of NP-SAS-PEG-NH_2 and its ability to serve as a potential T_2 contrast agent for MRI through relaxivity measurements, using a commercially available T_2 contrast agent Feridex IV (a dextran-coated iron oxide nanoparticle) serving as a reference (Fig. 4). The transverse relaxivity (slope of R_2) of NP-SAS-PEG-NH_2 is 339 $mM^{-1}\cdot s^{-1}$, which is 45% higher than that of Feridex IV.

In conclusion, we have introduced a new surface engineering approach to produce functionalized iron oxide nanoparticles. The functionalized hydrophilic nanoparticles exhibit strong magnetic relaxivity, excellent long-term colloidal stability in various biological media and negligible non-specific uptake by macrophages. The improved stability and biocompatibility can be attributed to the presence of the highly dense and stable PEG coating created via the strong affinity of SAS to oxide surfaces and the formation of siloxane bonds between PEG chains. The nanoparticles bear amine and carboxylic groups and are capable of conjugation of a wide variety of biomolecules for intended applications. While iron oxide nanoparticles are one of the most studied nanoparticle systems for biomedical applications, the surface engineering approach introduced here can be applied to any nanoparticles with an oxide surface (either native or oxidized).

Experimental Section

Materials

All general chemicals, unless otherwise specified, were purchased from Sigma-Aldrich (St. Louis, MO). Acetone and hexane were purchased from EMD (San Diego, CA). SAS was purchased from Gelest (Morrisville, PA). *N*-Succinimidyl iodoacetate (SIA), SPDP and tris(2-carboxyethyl) phosphine hydrochloride (TCEP·HCl) were purchased from Molecular Bioscience (Boulder, CO). PBS, DMEM, FBS and agarose were obtained from Invitrogen (Carlsbad, CA). RGD peptide cyclo(Arg-Gly-Asp-D-Tyr-Glu) was purchased from Peptide International (Louisville, KY). Sephacryl S-200 resin was purchased from GE Healthcare (Piscataway, NJ). PEG-bis(amine) (H_2N-PEG-NH_2) were synthesized according to a published procedure (starting material: PEG-diol, MW 2,000).[24] RAW246.7 cell lines were purchased from ATCC (Manassas, VA).

Synthesis of NP-SAS-PEG-NH_2

Oleic acid coated magnetite nanoparticles (NP-OA) were synthesized via thermal decomposition of iron oleate complex.[5] To a 5 ml of toluene solution containing 50 mg (iron content) of NP-OA, 40 mL of acetone was added, and the nanoparticles were collected by centrifugation. The nanoparticles were redispersed in 50 mL anhydrous toluene and transferred to a three-neck flask equipped with a heater. After the system was sealed and purged with nitrogen, 0.15 mL of SAS was injected, and the solution was heated to 100°C for 12 hours. The nanoparticles were precipitated by the addition of hexane, and collected using a rare earth magnet. The nanoparticles were washed twice with hexane and redispersed in anhydrous tetrahydrofuran (THF). To this solution, 100 mg of H_2NPEG-NH_2 and 2.5 mg of N,N′-dicyclohexylcarbodiimide (DCC) were added, and the reaction mixture was sonicated in a sonication bath for 12 hrs at 25°C. The nanoparticles was precipitated by the addition of 200 mL of hexane, and collected using a rare earth magnet. The precipitated nanoparticles were redispersed in 50 mL of anhydrous THF, and 250 mg of PEG-bis(amine) and 12.5 mg of DCC were added. The reaction mixture was kept in a sonication bath for 16 hrs at 25°C. The resulting product was precipitated by the addition of hexane, and collected using a rare earth magnet. After two additional cycles of THFredispersion and ether-precipitation, the residue solvent was evaporated and the nanoparticles were redispersed in 5 mL PBS. After passing through a 0.2 μm syringe filter, the nanoparticles were purified through gel filtration chromatography by Sephacryl S-200 column. The nanoparticles were stored in 0.1 M sodium bicarbonate buffer (pH 8.5). The concentration of nanoparticles was determined by inductively coupled plasma atomic emission spectroscopy (ICP-AES).

Conjugation of RGD Peptide

RGD peptide was conjugated to the NP-SAS-PEG-NH2 through haloacetyl crosslinking chemistry. NP-SAS-PEG-NH2 was first functionalized with iodoacetyl groups. Specifically,

5 mg of SIA was dissolved in 100 μL of anhydrous DMSO, and was then added to 2 ml of NP-SAS-PEG-NH2 (2.5 mg Fe/mL) suspended in 0.1 M sodium bicarbonate (pH 8.5). The resulting solution was allowed to react for 2 hrs. Excess succinimidyl iodoacetate (SIA) was removed from the suspension through gel chromatography using Sephacryl S-200 column equilibrated with 0.1 M sodium bicarbonate, 5 mM EDTA buffer at pH 8.0. RGD peptide was then added to the SIA modified nanoparticle solution, and the mixture was allowed to react for overnight at 4°C. Unreacted RGD was removed from the suspension using Sephacryl S-200 column equilibrated with PBS.

Nanoparticle Characterization

TEM samples were observed on a Phillips CM100 TEM (Philips, Eindhoven, The Netherlands) operating at 100 KV. FTIR spectra (resolution: 4 cm^{-1}) were acquired using a Nicolet 5DXB spectrometer (Thermo Scientific, Boston, MA). 2 mg of nanoparticle powder was mixed with KBr (Sigma-Aldrich, St. Louis, MO) and milled, and the mixture was pressed into a pellet for analysis. XPS experiments were performed by the National ESCA and Surface Analysis Center for Biomedical Problems at the University of Washington (Seattle, WA). XPS spectra of dried nanoparticle samples were obtained using a Surface Science Instrument X-probe spectrophotometer with a monochromatized Al X-ray source and 5 eV flood gun for charge neutralization. X-ray spot size for the acquisition was of the order of 800 μm, and the take-off angle was 55°. Pressure in the analytical chamber during the acquisition was less than 5×10^{-9} Torr. The dried nanoparticle powder was prepared in the way similar to FTIR sample preparation. The hydrodynamic size of nanoparticles was obtained via DLS using a Malvern Nano Series ZS particle size analyzer (Worcestershire, UK). The iron concentration of nanoparticle samples was 200 μg/mL.

Magnetic Properties by MRI

T_2 relaxation measurements were performed on a 4.7-T Bruker magnet (Bruker Medical Systems, Karlsruhe, Germany) equipped with Varian Inova spectrometer (Varian, Inc., Palo Alto, CA). Samples of NP-SAS-PEG-NH_2 and Feridex IV (Advanced Magnetics Inc., Cambridge, MA) were suspended in 1% agarose at concentrations of 0, 1.25, 2.5, and 5 μg Fe/ml. A 5 cm volume coil and spin-echo imaging sequence were used to acquire T_2-weight images of the nanoparticle samples. Images were acquired using a repetition time (TR) of 3000 ms and echo times (TE) of 13.6, 20.0, 40.0, 60.0, 80.0 and 100.0 ms. The spatial resolution parameters were: acquisition matrix of 256 × 128, field-of-view of 35 × 35 mm, section thickness of 1 mm and two averages. The T_2 map was generated by NIH ImageJ (Bethesda, MD) based on the equation, $SI = A \cdot \exp(-TE/T_2) + B$, where SI is the signal intensity, TE is the echo time, A is the amplitude, and B is the offset. R_2 map was generated by taking the reciprocal of T_2 map.

Macrophage Uptake Assay

RAW 264.7 were cultured in DMEM with 10% FBS and 1% antibiotics in 12-well plate. Cells were seeded at 0.5 million per well one day before the assay. The cells were washed twice with PBS, and then various types of nanoparticles in culture media (concentration 10 μg Fe/mL) were added. Cells incubated without nanoparticles were used as control. After 4 hr incubation at 37°C, 5% CO_2, the cells were washed three times with PBS, and lysed with 400 μL of 50 mM NaOH solution. Intracellular iron content was determined by quantifying iron content by the colorimetric ferrozine-based assay and determining cell count by protein quantification. [25]

Supplementary Material

Refer to Web version on PubMed Central for supplementary material.

References

1. Peer D, Karp JM, Hong S, Farokhzad OC, Margalit R, Langer R. Nature Nanotechnol 2007;2:751–760. [PubMed: 18654426]
2. Sun C, Lee JSH, Zhang M. Adv. Drug Deliv. Rev 2008;60:1252. [PubMed: 18558452]
3. Cai WB, Chen XY. Small 2007;3:1840–1854. [PubMed: 17943716]
4. Weissleder R, Pittet MJ. Nature 2008;452:580–589. [PubMed: 18385732]
5. Park J, An K, Hwang Y, Park J-G, Noh H-J, Kim J-Y, Park J-H, Hwang N-M, Hyeon T. Nat. Mater 2004;3:891–895. [PubMed: 15568032]
6. Sun S, Zeng H, Robinson DB, Raoux S, Rice PM, Wang SX, Li G. J. Am. Chem. Soc 2004;126:273–279. [PubMed: 14709092]
7. Moghimi SM, Hunter AC, Murray JC. FASEB J 2005;19:311–330. [PubMed: 15746175]
8. Jun, Y. w.; Huh, YM.; Choi, J. s.; Lee, JH.; Song, HT.; Kim, S. j.; Yoon, S.; Kim, KS.; Shin, JS.; Suh, JS.; Cheon, J. J. Am. Chem. Soc 2005;127:5732–5733. [PubMed: 15839639]
9. Yu WW, Chang E, Falkner JC, Zhang J, Al-Somali AM, Sayes CM, Johns J, Drezek R, Colvin VL. J. Am. Chem. Soc 2007;129:2871–2879. [PubMed: 17309256]
10. Figuerola A, Fiore A, Di Corato R, Falqui A, Giannini C, Micotti E, Lascialfari A, Corti M, Cingolani R, Pellegrino T, Cozzoli PD, Manna L. J Am Chem Soc 2008;130:1477–1487. [PubMed: 18181628]
11. Veiseh O, Sun C, Gunn J, Kohler N, Gabikian P, Lee D, Bhattarai N, Ellenbogen R, Sze R, Hallahan A, Olson J, Zhang MQ. Nano Letters 2005;5:1003–1008. [PubMed: 15943433]
12. Zhang Y, Kohler N, Zhang MQ. Biomaterials 2002;23:1553–1561. [PubMed: 11922461]
13. Zhang Y, Sun C, Kohler N, Zhang MQ. Biomedical Microdevices 2004;6:33–40. [PubMed: 15307442]
14. Kohler N, Fryxell GE, Zhang MQ. Journal of the American Chemical Society 2004;126:7206–7211. [PubMed: 15186157]
15. Sun C, Veiseh O, Gunn J, Fang C, Hansen S, Lee D, Sze R, Ellenbogen RG, Olson J, Zhang M. Small 2008;4:372–379. [PubMed: 18232053]
16. Veiseh O, Sun C, Gunn J, Kohler N, Gabikian P, Lee D, Bhattarai N, Ellenbogen R, Sze R, Hallahan A, Olson J, Zhang M. Nano Letters 2005;5:1003–1008. [PubMed: 15943433]
17. Sun C, Lee JS, Zhang M. Adv Drug Deliv Rev 2008;60:1252–1265. [PubMed: 18558452]
18. Xie J, Xu C, Kohler N, Hou Y, Sun S. Adv. Mater 2007;19:3163–3166.
19. Ferrari M. Nature Reviews Cancer 2005;5:161–171.
20. Willis AL, Turro NJ, O'Brien S. Chem. Mater 2005;17:5970–5975.
21. Pouchert, CJ.; Aldrich Chemical, C. The Aldrich library of FT-IR spectra. Aldrich Chemical Co.; Milwaukee, Wis.: 1985.
22. Schellenberger EA, Sosnovik D, Weissleder R, Josephson L. Bioconjugate Chem 2004;15:1062–1067.
23. Petri-Fink A, Steitz B, Finka A, Salaklang J, Hofmann H. Eur. J. Pharm. Biopharm 2008;68:129–137. [PubMed: 17881203]
24. Ranucci E, Ferruti P. Synth. Comm 1990;20:2951–2957.
25. Riemer J, Hoepken HH, Czerwinska H, Robinson SR, Dringen R. Analytical Biochemistry 2004;331:370–375. [PubMed: 15265744]

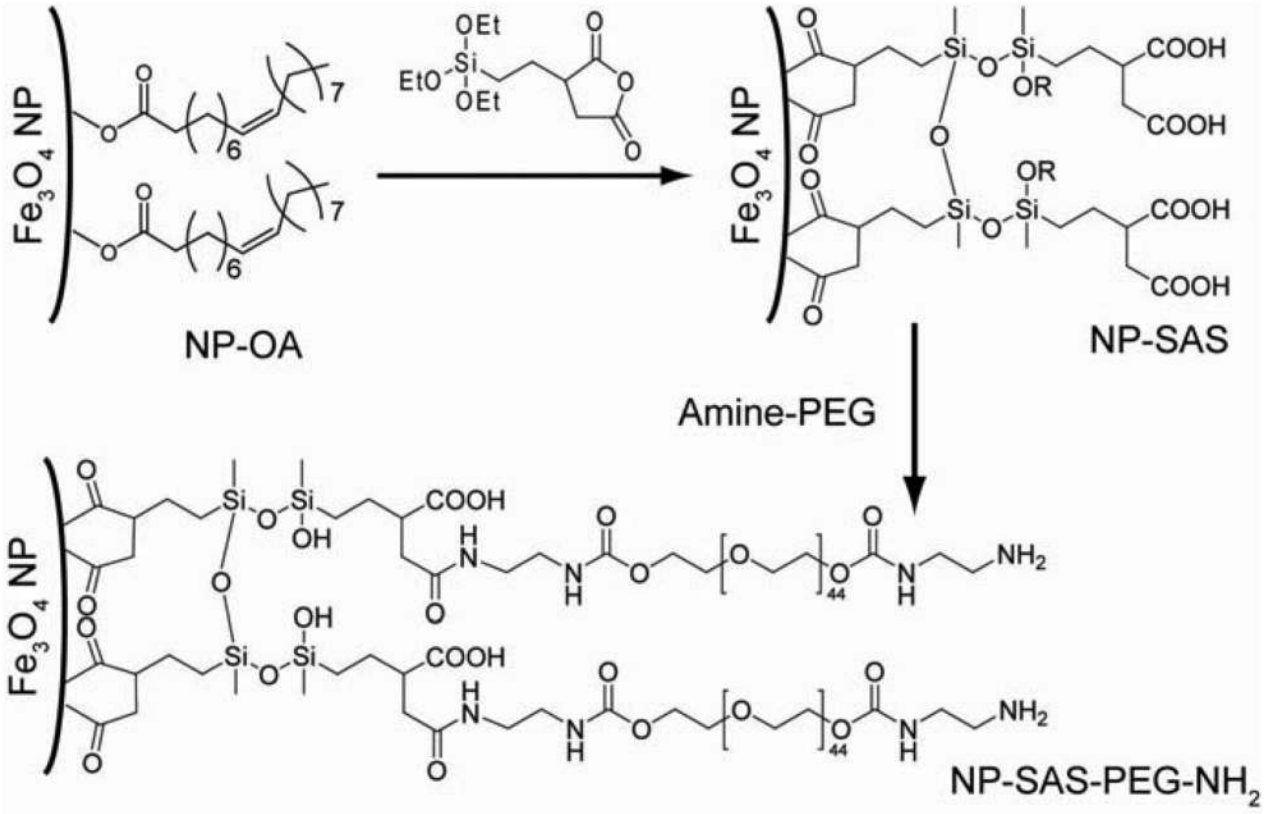

Scheme 1.
Schematic of nanoparticle surface modification.

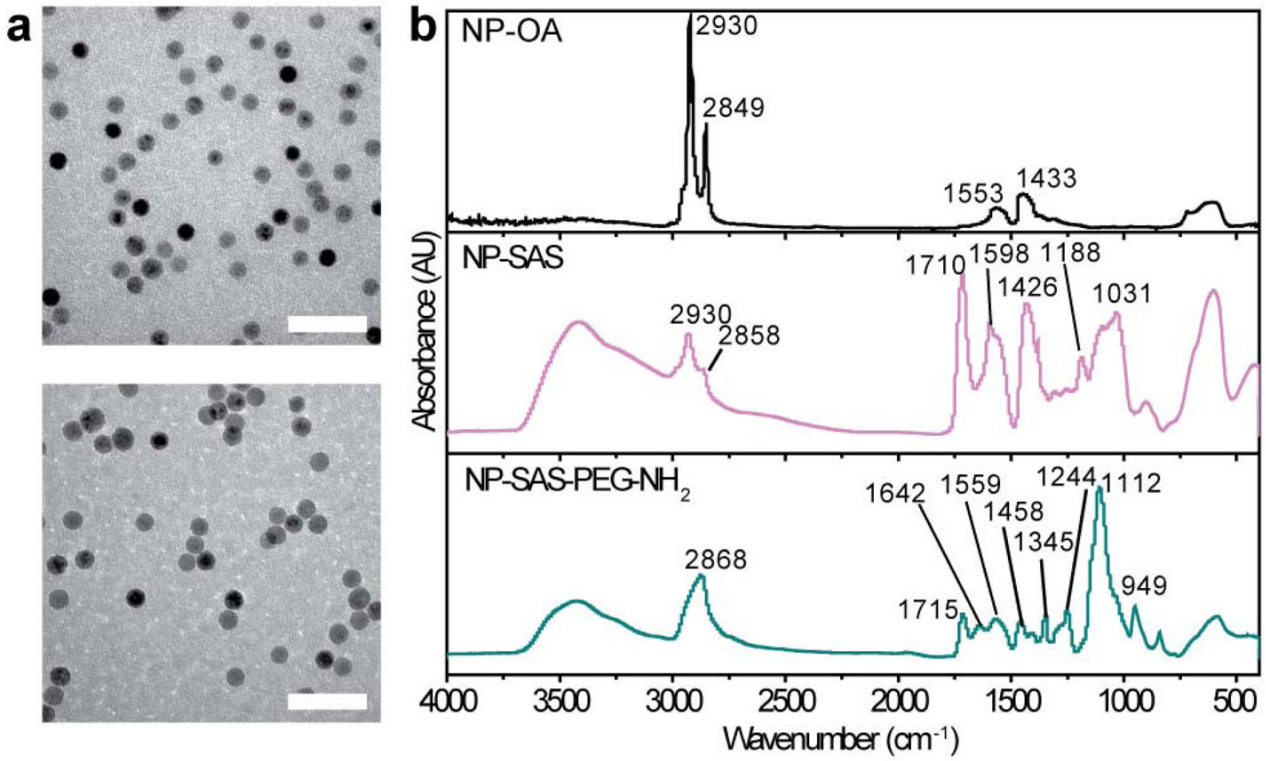

Figure 1.

(a) TEM images of oleic acid-coated nanoparticles (top) and NP-SAS-PEG-NH_2 (bottom). Scale bar: 60 nm. (b) FTIR spectra of oleic acid-coated nanoparticles, NP-SAS, and NP-SAS-PEG-NH_2.

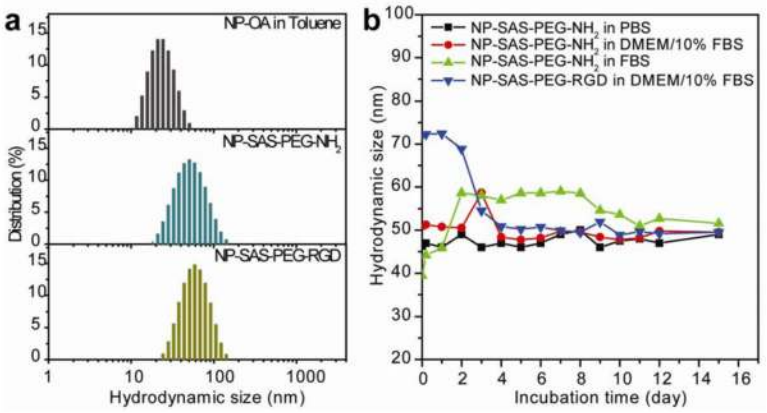

Figure 2.

Colloidal properties of iron oxide nanoparticles: (a) Hydrodynamic size of nanoparticles (from top to bottom): oleic acid-coated nanoparticles in toluene, NP-SAS-PEGNH_2 in PBS, and NP-SAS-PEG-RGD conjugates in PBS. (b) Long-term stability study of NPSAS-PEG-NH_2 in various media. The stability of NP-SAS-PEG-RGD conjugates in DMEM with 10% FBS is also included.

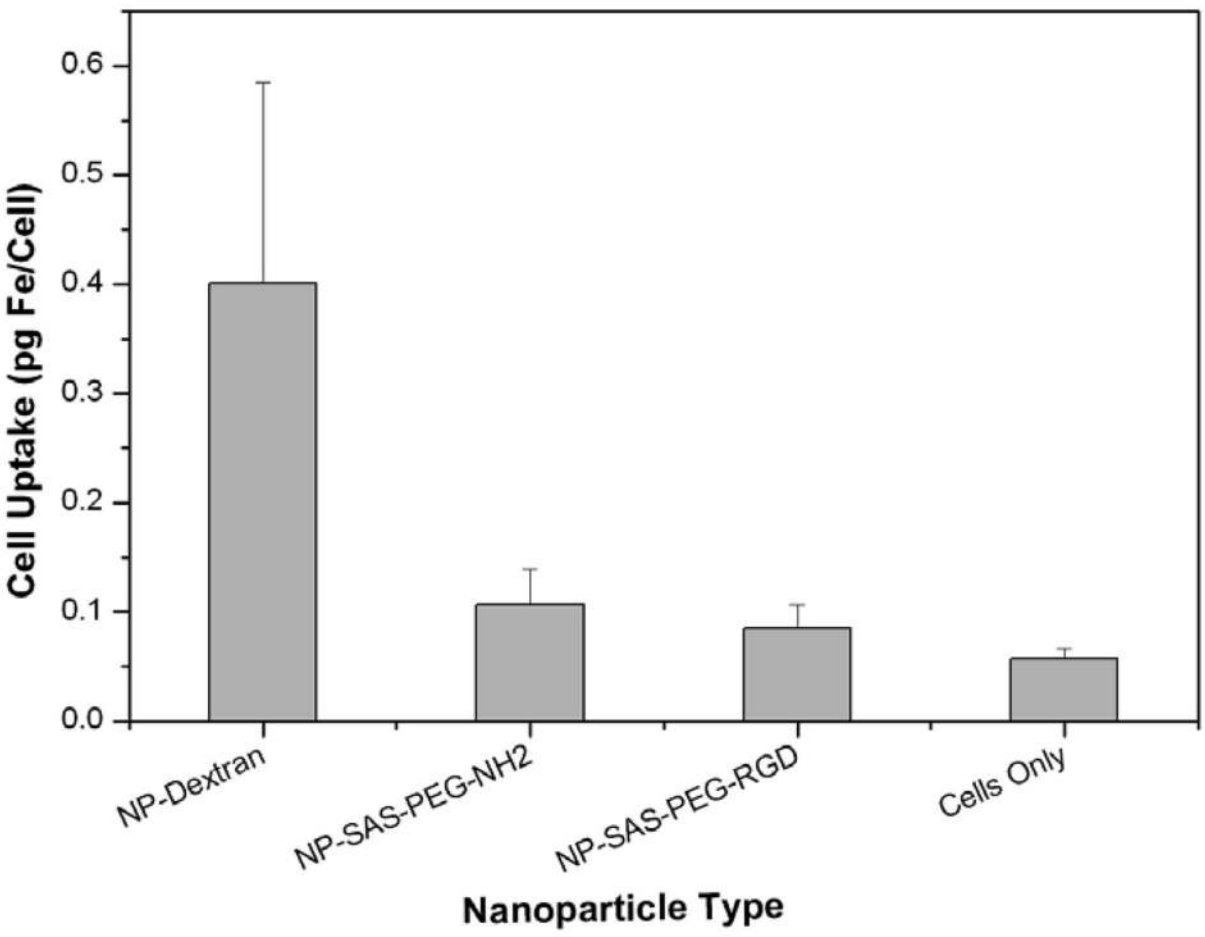

Figure 3.
Intracellular iron content determined by macrophage uptake assay. All nanoparticles were incubated at 10 μg Fe/mL.

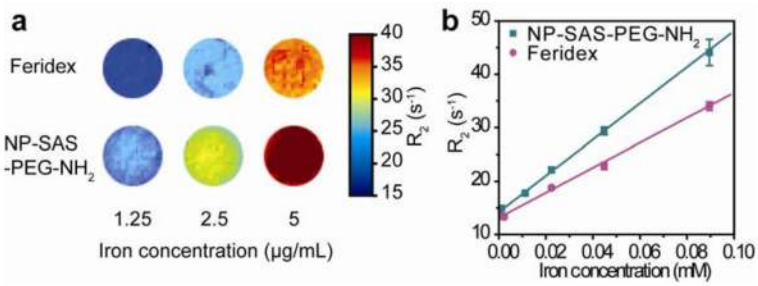

Figure 4.

Relaxation properties of NP-SAS-PEG-NH_2 vs. Feridex, characterized by MRI: (a) Colorized R2 maps of gel phantoms containing either NP-SAS-PEG-NH_2 or Feridex at different iron concentrations. (b) R_2 relaxation rates as a function of iron concentration for both NP-SAS-PEG-NH_2 and Feridex. Error bars represent variation in measurement of a circular region of interest 3 mm in diameter.